PCCP

Detection of ligand binding to glycopolymers using Saturation Transfer Difference NMR

Journal:	*Physical Chemistry Chemical Physics*
Manuscript ID	CP-ART-07-2021-003410.R2
Article Type:	Paper
Date Submitted by the Author:	17-Sep-2021
Complete List of Authors:	Basu, Amit; Brown University, Chemistry Department Muzulu, Janet; Brown University, Chemistry Department

ARTICLE

Detection of ligand binding to glycopolymers using Saturation Transfer Difference NMR

Received 00th January 20xx,
Accepted 00th January 20xx

DOI: 10.1039/x0xx00000x

Janet Muzulu[a] and Amit Basu*[a]

We report the use of Saturation Transfer Difference (STD) NMR spectroscopy to observe the interaction of various phenylboronic acids (PBAs) with synthetic glycopolymers presenting galactose and glucose. After optimizing experimental parameters to maximize spin diffusion within the glycopolymers, STD NMR experiments were successfully used to detect binding of PBAs to the polymers. Amplification factor build-up curves in conjunction with differential epitope mapping experiments were used to generate an epitope map for the bound boronic acids. STD NMR was also used to detect the interaction between indole and a galactosylated glycopolymer, providing an indole-based view of this C*H*–π interaction, a common binding motif in carbohydrate recognition.

Introduction

Modern NMR experiments provide powerful tools for detecting and characterizing protein – small molecule interactions, and provide information regarding binding affinity as well as identifying protons on the small molecule ligand in close contact with the protein – i.e. the binding epitope.[1-4] Several of these experiments, such as saturation transfer difference (STD) spectroscopy, are based on detecting signals from the small molecule ligand and rely on the large difference in molecular weight between the protein and the ligand. Non-proteinogenic macromolecules can also be used as the macromolecular 'receptor' for STD-NMR experiments, but these applications have not been as widely developed, and there are only a handful of reports describing the extension of this experiment to other macromolecular systems.

STD-NMR has been used to study the binding of small molecules to non-proteinogenic macromolecules such as chromatographic supports,[5,6] inorganic and organic nanoparticles,[7-11] lipid nanodiscs,[12] nucleic acids,[13-15] organic pigments,[16] polysaccharides,[17] and even a glycosylated natural product.[18] In many of these cases, saturation transfer was solely used to confirm the binding of a ligand to the macromolecule without determining an epitope map or binding constant for the interaction. Saturation transfer from a single-chain cross-linked nanoparticle comprised of a polynorbornene backbone has been successfully carried out[11] but whether non-cross-linked linear polymers would be as effective in the STD-NMR experiment was not clear. Of more direct relevance is the observation of efficient saturation transfer from pectin, a linear polysaccharide that adopts a extended conformation, to bound anthocyanin natural products.[17] A recent report describes the use of STD NMR to confirm an interaction between a polyacrylamide glycopolymer and a 42-mer peptide.[19] To the best of our knowledge the use of STD NMR to generate epitope maps for polymer-bound ligands has not been reported to date. Given the numerous applications of polymers that involve their binding to smaller molecules – sensors, drug-delivery, excipients, etc. – the ability to probe ligand binding to polymers using STD NMR experiments would provide a valuable addition to the toolkit for studying polymer molecular recognition, as it can provide insights into ligand binding affinity and the orientation of the bound ligand, which is useful for improving affinity and selectivity.

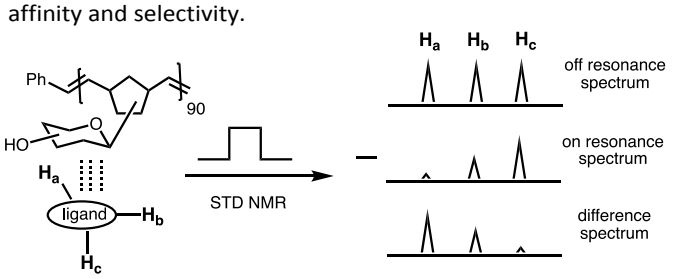

Figure 1 – Schematic of STD-NMR experiment and epitope mapping

The STD experiment involves the acquisition of two separate spectra, one obtained with on-resonance irradiation and the second with off-resonance irradiation.[20] For the on-resonance spectrum, resonances of the glycopolymer are selectively irradiated at a frequency where only receptor signals resonate. The resulting saturation spreads through the entire macromolecule by spin diffusion and is transferred to protons of the bound form of the ligand that are in close proximity to the macromolecular receptor. The off-resonance spectrum is a reference experiment in which the sample is irradiated at a frequency far removed from both the macromolecule and ligand resonances. A difference STD spectrum, generated by

[a] *Department of Chemistry, Brown University, Providence RI, USA 02912*
* abasu@brown.edu

Electronic Supplementary Information (ESI) available: [Detailed experimental procedures, characterization data, and additional spectral data]. See DOI: 10.1039/x0xx00000x

subtraction of the on-resonance spectrum from the off-resonance spectrum, exhibits signals for protons on the ligand that received saturation transfer from the macromolecule (Figure 1). The degree of saturation of individual ligand protons reflects their proximities to the receptor and can be used to obtain an epitope map that provides insight into the ligand orientation when it is bound to the receptor.

We asked if soluble polymers could serve as efficient sources of saturation transfer and be used to generate epitope maps for polymer-bound low molecular weight ligands. To address this question, we examined the interaction of glycopolymers with phenyl boronic acids (PBAs). Glycopolymers mimic natural multivalent presentations of carbohydrates such as mucins and proteoglycans and are widely used to study carbohydrate recognition.[21-23] PBAs bind monosaccharides with mM or high μM affinity via the formation of reversibly-linked boronate esters,[24-26] and provide a robust probe for developing a polymer-based STD NMR experiment.

We report here the use of STD NMR to observe the interaction of various substituted PBAs with glycopolymers functionalized with either galactose or glucose. Optimization of experimental parameters required the application of differential epitope mapping STD NMR in order to obtain a clear epitope map for the bound boronic acid. We also report the use of STD NMR to detect the interaction of indole with a glycopolymer via non-covalent CH–π interactions.[27,28] This work describes a new tool for detecting small molecule binding to polymers.

Results and Discussion

Optimization of Spin Diffusion and Saturation Transfer

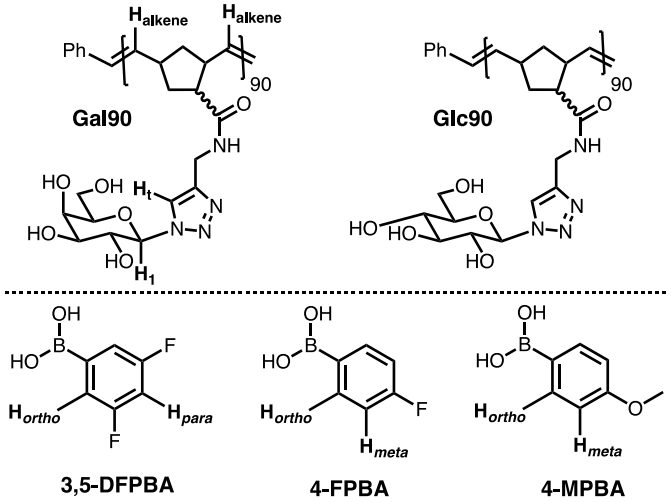

Figure 2 – Structures of PBAs and glycopolymers used in these studies

The galactose-functionalized glycopolymer **Gal90** (Figure 2) was prepared as previously reported (see Supporting Information Figures S1 – S5).[29] Briefly, ring opening metathesis polymerization of the NHS ester of norbornene carboxylic acid was followed by reaction of the poly-ester with propargyl amine to provide a poly-alkyne. Subsequent reaction of the poly-alkyne with a 1-azidosugar using a copper-promoted click reaction afforded the polymer. Galactose contains a 1,2 *cis* diol functionality that is optimal for PBA binding. A polymer (**Glc90**) which lacks the *cis* diol, and does not bind to PBAs as strongly as galactose,[30,31] was prepared as a control.

Optimal parameters for maximal saturation of **Gal90** were determined by varying the on-resonance frequency, pulse shape, pulse length, and pulse power, all at a fixed saturation time of 1 s. The glycopolymer ^{1}H NMR spectrum exhibits numerous resonances between 5 ppm and 0.8 ppm (top spectrum, Figure 3), a region outside of the spectral window of the PBAs, providing a wide window for selection of the on-resonance saturation frequency. Efficient spin diffusion within the macromolecule leads to the saturation of resonances throughout the entire macromolecule and not just at site of irradiation.[20] Glycopolymers have high proton density along the polymer backbone, which should allow spin diffusion through a dipolar-coupled network of spins in the macromolecule. Unlike STD-NMR with proteins, where the saturated resonances typically correspond to methyl groups in the interior of the folded protein, saturation of protons that are more solvent accessible can result in loss of STD signal from saturation transfer to water. Nonetheless the success of STD-NMR with receptors such as nucleic acids and polysaccharides which have many solvent accessible and solvent exchangeable protons suggests that effective STD-NMR experiments can be carried when sufficient spin density is present.[32,33] Our first objective, therefore, was to determine and optimize the ability of the glycopolymers to be effectively saturated and undergo spin diffusion.

A reference spectrum (Figure 3) was obtained by conducting an off-resonance experiment with a saturation frequency far removed from **Gal90** resonances (40 ppm). The reference spectrum exhibits the broad resonances of the glycopolymer, along with smaller sharp peaks corresponding to low molecular weight impurities. I_0 is defined as the intensity of the triazole peak at 8.05 ppm in the reference spectrum. The on-resonance experiment was conducted using on-resonance saturation frequencies located in the aliphatic region of **Gal90,** and triazole proton intensities (I_{SAT}) in the corresponding spectra were obtained. If the resulting difference spectrum (off-resonance spectrum – on-resonance spectrum) exhibited an envelope similar to that of the reference spectrum, which occurs when $I_{SAT} << I_{0,}$ this indicated that effective intra-polymer spin diffusion was occurring.[20] If the difference spectrum generated a flat line, (i.e. $I_{SAT} \approx I_0$), this indicated that efficient spin diffusion was not occurring, and no STD effect was observed. The STD effect is calculated using equation 1.[34]

$$\text{STD effect} = \frac{I_0 - I_{SAT}}{I_0} \qquad [1]$$

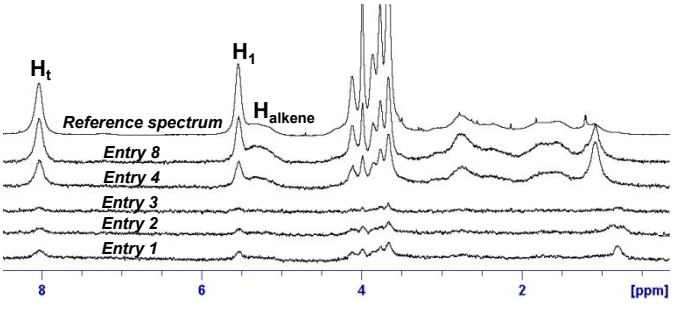

Figure 3 – The envelopes of the **Gal90** STD spectra are similar to that of the reference spectrum, indicating that the glycopolymer is effectively saturated. Experimental details for each entry are found in Table 1. All spectra are shown at the same vertical scale, with the exception of the reference spectrum, shown at 0.15x scale. H_t – triazole proton; H_1 – anomeric proton, H_{alkene} – polymer alkene protons – see Figure 2

Table 1. Optimization of selective excitation parameters to maximize the STD effect of **Gal90**

Entry	Pulse shape	Pulse power [-dB]	Pulse length [ms]	Saturation frequency [ppm]	STD effect
1	Gauss	50	50	0.8	0.034
2	E-burp	50	50	0.8	0.022
3	Reburp	50	50	0.8	0.011
4	Gauss	50	50	1.07	0.090
5	E-burp	50	50	1.07	0.061
6	Reburp	50	50	1.07	0.028
7	Gauss	47.5	25	0.8	0.058
8	Gauss	47.5	25	1.07	0.130
9	Gauss	47.5	10	1.07	0.129
10	Gauss	70	25	1.07	0
11*	Gauss	47.5	25	1.07	0.098

Saturation time = 1 s. Off-resonance irradiation was applied at 40 ppm. *A $T_{1\rho}$ spin lock filter of 50 ms was applied.

The suggested parameters from the NMR vendor§ using a Gaussian shaped pulse (Gauss) of 50 ms length and pulse power of -50 dB resulted in an STD effect of 0.034 upon irradiation at 0.8 ppm (Table 1 Entry 1 & Figure 3). Changing the pulse shape to E-burp or Reburp decreases the STD effect (Table 1 Entries 2/3, & Figure 3). Changing the on-resonance frequency to 1.07 ppm results in a 3-fold increase in the STD effect, with a Gauss-shaped pulse as the most effective (Table 1 Entries 4-6 & Figure 2). Using a shorter pulse length (25 ms) results in a larger STD effect. At either on-resonance frequency (Table 1 Entries 7,8), the STD effect is almost 1.5 times greater than a 50 ms pulse (Entry 4 vs. 8). This observation is consistent with prior reports that pulses shorter than 50 ms can result in stronger STD effects.[35] The use of a 10 ms Gauss pulse marginally reduces the STD effect, and the use of a low power pulse -70 dB results in no detectable spin diffusion (Table 1, Entries 9, 10). When a $T_{1\rho}$ spin lock filter of 50 ms was applied to the parameters of Entry 8 (25 ms Gauss pulse), the STD effect dropped from 0.130 to 0.098 (Entry 11 & Figure S6). The spin lock filter suppresses the broad resonances of the macromolecule in order to allow the small molecule resonances to be more clearly observed and to quantitate their intensities without interference from any overlapping macromolecule resonances.[34] The parameters in entry 11 were adopted for all subsequent experiments.

STD-NMR of Glycopolymer-PBA binding

With optimized parameters in hand, the interaction of 3,5-difluorophenylboronic acid (3,5-DFPBA) with **Gal90** was examined using STD NMR. As a negative control, irradiation of 3,5-DFPBA using these parameters did not elicit an apparent STD effect, confirming that no ligand resonances were excited by the on-resonance pulse (Figure S7, spectra G & I). Stacked STD plots of a solution of 3,5-DFPBA (1 mM) in the presence of **Gal90** (100 μM) in PBS buffer (100 mM, pH 7.2) at saturation times varying from 1 to 8 seconds are shown in Figure 4. These plots display an increase in peak intensities of the aromatic resonances of 3,5-DFPBA with increasing saturation time. This observation indicates that the PBA is undergoing saturation transfer from the **Gal90**, since the earlier control experiment had established that no ligand resonances are directly excited by the pulse sequence used in the experiment. Figure 4 shows that **Gal90** resonances receive insufficient background suppression as exemplified by the observation of the triazole proton resonance from the glycopolymer. Incomplete receptor suppression is often observed at low ligand concentrations.[13,36] Nevertheless, the signals from 3,5-DFPBA can still be readily quantified since they are well resolved from the **Gal90** triazole resonance.

Figure 4 – Representative STD spectra of 3,5-DFPBA (1 mM) in the presence of **Gal90**

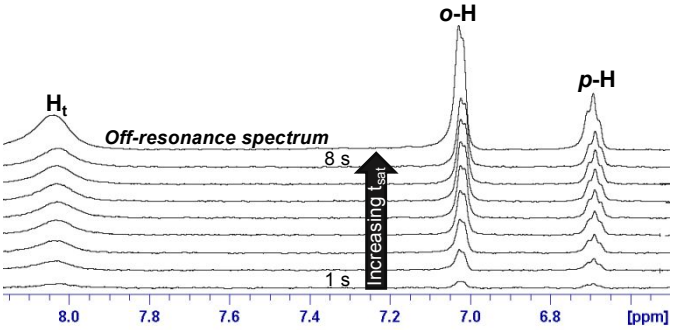

(100 μM) in PBS buffer (100 mM, pH 7.2). Intensity of the small molecule peaks increases with increasing saturation time (t_{sat}). The reference spectrum is scaled x0.7 relative to the STD spectra.

The STD amplification factor (STD-AF) allows a better assessment of the absolute magnitude of the STD effect, and can be quantified by multiplying equation 1 by the ligand to receptor ratio:[37]

$$STD\text{–}AF = \frac{I_0 - I_{SAT}}{I_0} \times \frac{[L]}{[R]} \quad [2]$$

where [L] is the PBA concentration and [R] is the glycopolymer concentration. Variations in the longitudinal relaxation times (T_1) of the small molecule ligand protons can generate artifacts in epitope mapping. Protons with longer T_1 relaxation times accumulate saturation in solution and exhibit higher STD relative intensities, overestimating their proximity to the macromolecule.[37] Generation of STD buildup curves using multiple saturation times is used to eliminate the T_1 bias at long saturation times. The build-up curves are fitted to equation 3.

$$STD\text{–}AF_{tsat} = STD\text{–}AF_{max}(1 - e^{-k_{sat} \times t_{sat}}) \quad [3]$$

The term STD-AF_{max} corresponds to the plateau of each curve, k_{sat} is a rate constant that measures the speed of STD build-up, and t_{sat} is the saturation time. Values for k_{sat} and STD-AF_{max} are derived by least-squares fitting, and their product yields the initial slope of the build-up curve at zero saturation time, STD-AF_0, a term that corresponds to the STD intensity without any T_1 bias. The ligand protons that are positioned closest to the saturated receptor protons exhibit the largest amplification

factors, as they experience a greater degree of saturation transfer from the macromolecule. The amplification factor for these protons is set to 100%, and the amplification factors for all other ligand protons are scaled relative to it. The resulting percentages provide an epitope map[§§] of the small molecule, where lower values correspond to decreased proximity of those ligand protons to the receptor.

The STD-AF of both the *ortho* and *para* protons of 3,5-DFPBA increases with saturation time and begins to level off at a saturation time of 8 s (Figure 5A, purple curves). Curve-fitting of Equation 3 to these plots to determine STD-AF_0 values provided values of 0.69 and 0.88, for the *ortho* and *para* protons respectively (Tables S1 & S2). This observation was unexpected, since the *ortho* protons are more proximal to the boronate ester that links the PBA to the glycopolymer and should exhibit a stronger STD effect. We speculated that the *para* proton may be oriented closer to the hydrocarbon backbone than the *ortho* protons are, resulting in more effective saturation transfer to the former. If so, saturation of glycopolymer protons situated closer to the bound boronic acid (i.e. ring protons of the sugar) should provide a different epitope map. We carried out a differential epitope mapping (DEEP) STD NMR experiment to test this hypothesis.[14,38]

DEEP STD-NMR

Differential epitope mapping (DEEP) STD NMR is an extension of the STD NMR method which allows the orientation of small molecules bound to receptors to be defined through selective saturation of different sets of macromolecular protons.[14,38] The intensity changes in the ligand signals in an STD NMR experiment are dependent on the location of the saturated macromolecular protons with respect to the ligand protons.[39] When spin diffusion is inefficient in the macromolecule due to exchange-mediated leakage, differences in ligand epitope maps are observed if STDs are acquired at different on-resonance frequencies.

After confirming effective spin diffusion (Figures S9 & S10) of **Gal90** upon on-resonance irradiation at 3.75 ppm, where the carbohydrate protons of the glycopolymers resonate, we carried out STD NMR experiments with the **Gal90•**3,5-DFPBA mixture. The *ortho* and *para* protons of 3,5-DFPBA exhibited larger STD-AFs in the presence of **Gal90**, with STD-AF_0 values of 1.33 and 1.19 respectively (Figure 5A, blue curves). These values are higher than those obtained when the aliphatic protons of **Gal90** were irradiated. More significantly, the values reverse the epitope map for the PBA protons (Tables S3 & S4). This data indicates that the *ortho* protons of polymer-bound 3,5-DFPBA are positioned closer to the carbohydrate moieties of **Gal90**, while the *para* proton of the bound 3,5-DFPBA is situated in closer proximity to the aliphatic protons of **Gal90**, since the latter exhibit larger STD-AF values upon irradiation at 1.07 ppm. These results indicate the importance of carrying out DEEP-STD NMR, especially when using macromolecules that are not as globular as traditional proteins.[38,39]

Variation in PBA

The binding affinity of PBAs for carbohydrates is dependent on numerous factors, including buffer identity and *p*H, *p*K_a values of both the sugar hydroxyl group and the boronic acid, as well as the stereochemistry of the sugar diols.[40,41] STD NMR experiments with 4-fluorophenylboronic acid (4-FPBA) and 4-methoxyphenylboronic acid (4-MPBA) in the presence of **Gal90** also exhibited an STD effect, although with lower intensities than those for 3,5-DFPBA (Figure 5A, orange and red curves).[§§§] This observation is consistent with lower binding constants for both 4-FPBA and 4-MPBA as a result of their higher *p*K_a values (8.8[42] and 9.4[43] respectively) compared to 3,5-DFPBA (7.1[42]). In both of these cases, the *ortho* protons exhibit the larger STD-AF_0, but only marginally higher than the *meta* protons (Tables S3 & S4).[§§§§]

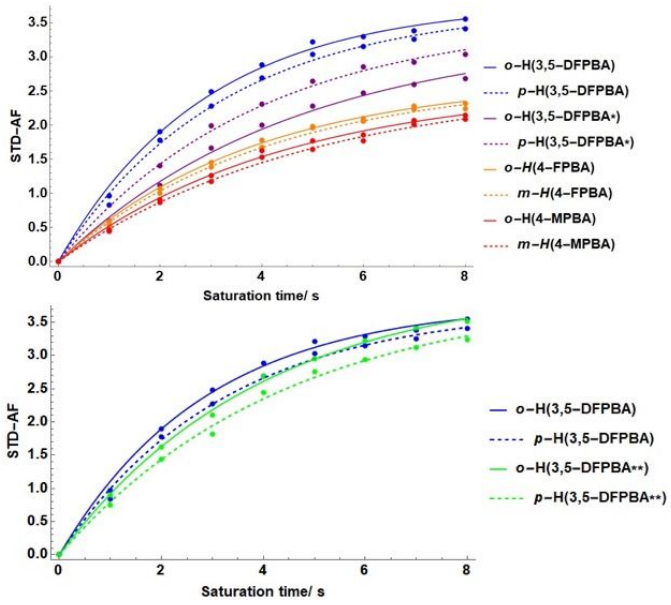

Figure 5 – STD build-up curves for the PBAs (1 mM) in the presence of glycopolymers (100 μM). A – Build up curves for 3,5-DFPBA in the presence of **Gal90**. Blue curves: Data obtained upon on-resonance irradiation at 3.75 ppm. Purple curves: *Data obtained upon on-resonance irradiation at 1.07 ppm. Orange and red curves: 4-FPBA and 4-MPBA respectively in the presence of **Gal90** after on-resonance irradiation at 3.75 ppm. B – Data obtained upon on-resonance irradiation at 3.75 ppm. Green curves: **Build-up curves for 3,5-DFPBA in the presence of **Glc90**.

Similarly, boronic acids bind with lower affinity to glucopyranosides, which lack the *cis* diol present in galactose.[30,31] We determined the STD effect for 3,5-DFPBA with a glycopolymer bearing glucose (**Glc90**). We confirmed that spin diffusion occurs successfully in **Glc90** by monitoring the increase in the STD effect of the triazole proton with increasing saturation time (Figure S10). Conducting the STD NMR experiment of **Glc90** in the presence of 3,5-DFPBA indicates saturation transfer to protons of the 3,5-DFPBA. As expected, the STD-AF values for 3,5-DFPBA in the presence of **Glc90** (Figure 5B - green curves) are lower than those observed in the presence of **Gal90**, with STD-AF_0 values of 1.05 and 0.91 for the *ortho* and *para* protons respectively. As in the case with **Gal90**, the ordering of the *ortho* and *para* STD-AF_0 values is switched when the on-resonance saturation is carried out at 1.07 ppm (Figure S14). Additionally, 3,5-DFPBA exhibits larger amplification factors in the presence of **Gal90** than **Glc90**

regardless of the irradiation frequency, reflecting stronger binding to **Gal90**. These experiments illustrate how STD NMR can be effectively used to detect the interaction between boronic acids and glycopolymers, and that trends in the magnitude of the STD effects with different PBAs and glycopolymers mirror the expected changes in binding affinity.

DOSY NMR

Diffusion NMR (DOSY) experiments corroborated the STD NMR findings. Figure 6 displays the DOSY spectra of 3,5-DFPBA in the absence (red crosspeaks) and presence (blue cross peaks) of **Gal90**. 3,5-DFPBA diffuses much faster than the polymer, but exhibits a smaller diffusion constant in the presence of the polymer. The resonances of free 3,5-DFPBA in the absence of **Gal90** exhibit an average log D value of -9.27±0.02, as indicated by the red dotted line in Figure 6 (and Figure S19). In the presence of **Gal90**, 3,5-DFPBA exhibits an average log D value of -9.42±0.02 (blue dotted line, Figure 6), equating to a Δlog D (log D_{bound} – log D_{free}) of -0.15±0.03. The decrease in the log D value is consistent with complexation of 3,5-DFPBA with the glycopolymer.[44,45] The Δlog D of 3,5-DFPBA is -0.11±0.03 in the presence of **Glc90** (Figure S20). 4-FPBA and 4-MPBA exhibit Δlog D values of -0.09±0.01 and -0.07±0.05 respectively in the presence of **Gal90** (Figures S21 & S22). These Δlog D values follow the trend of binding affinities observed with STD NMR. Additional evidence for binding of 3,5-DFPBA to the carbohydrate moieties of **Gal90** was provided by a competition experiment (Figure S23). In the presence of a 100-fold excess of monovalent galactose, a Δlog D of -0.01 was observed. The small Δlog D indicates that the monosaccharide inhibits the PBA from interacting with the glycopolymer by successfully competing for the boronic acid.

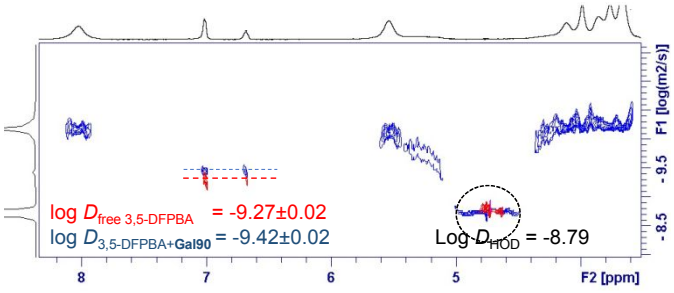

Figure 6 – DOSY 2D spectrum of (red): free 3,5-DFPBA (1 mM) and (blue): 3,5-DFPBA (1 mM) in the presence of **Gal90** (100 µM) in phosphate buffer (0.1 M) in D_2O, pH 7.2 at room temperature.

Indole – Sugar

While the results above clearly demonstrate that STD NMR experiments can detect the binding of PBAs to glycopolymers, this approach can also be extended to small molecules that interact non-covalently with glycopolymers. Aromatic amino-acid side-chains interact with galactose via CH–π interactions.[27,28] This interaction has been observed in sugar-bound protein crystal structures that indicate close proximity between ligand-derived galactose residues and the indole side-chain of tryptophan, as well as in NMR titrations of monosaccharides with indole and phenol.[46-48]

As an illustrative example, we carried out an STD NMR experiment with **Gal90** using indole as the small molecule ligand. The STD-AF buildup curves for the indole proton resonances as a function of saturation time are shown in Figure 7. Figure 7 indicates that indole interacts with **Gal90** given that its various resonances exhibit an increase in STD-AF with increasing saturation time. Negative control experiments in the absence of **Gal90** resulted in total signal cancellation of the indole resonances (Figure S24), confirming that the observed STD effect arises from saturation transfer from **Gal90** to the indole. The epitope map (Table S7) indicates a spatial preference for the galactose•indole interaction, as the amplification factors for H2 and H7 are smaller than those for the other protons in indole. We note that the STD-AF buildup curves for this interaction do not provide as smooth of a fit as observed with the PBAs, with a downward trend observed at longer saturation times, perhaps due to local heating effects. It is worth noting that this experiment provides an indole-centered perspective of this interaction, which has typically been examined by examining chemical shift perturbations in the carbohydrate.[46,47] We are examining the CH–π interaction of SGal in further details, and this work will be reported elsewhere in due course.

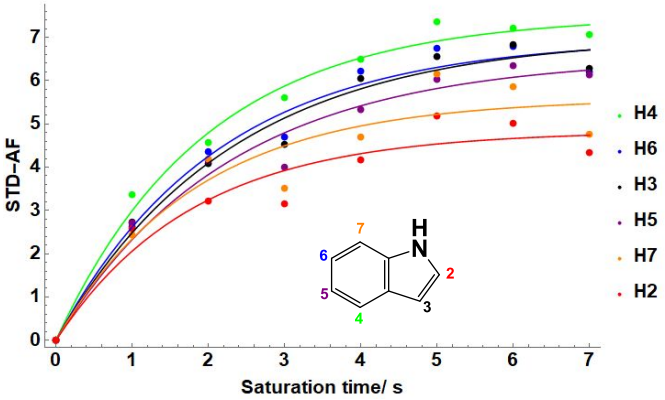

Figure 7 – STD build up curves showing that indole (3 mM) interacts with **Gal90** (50 µM) after on-resonance irradiation at 3.75 ppm. H4 exhibits the largest STD-AF at all saturation times while H2 exhibits the smallest STD-AF.

Conclusions

In this work, we have shown that glycopolymers can serve as the macromolecular component of an STD NMR experiment. Resonances on the polymer backbone and carbohydrate moieties can successfully be saturated, undergo spin diffusion, and transfer saturation to bound ligands. Small molecules such as PBAs or indole that interact with glycopolymers can receive this saturation from the glycopolymers and generate an interaction epitope map that provides additional information about the orientation of the ligand with respect to the glycopolymer. Variation in the saturation frequency using DEEP STD NMR provides additional details of the ligand receptor interaction that cannot be obtained using saturation at a single frequency. The interaction of various PBAs with glycopolymers has been detected using STD NMR and DOSY NMR. This work demonstrates the use of glycopolymers in STD NMR studies to

generate epitope maps for ligand-binding. The techniques described here can be applied to investigate and quantify the binding affinities of other polymers with small molecules.[49-51]

Author Contributions

JM and AB designed experiments, JM carried out experiments, and JM and AB analyzed results and wrote the manuscript.

Conflicts of interest

There are no conflicts to declare.

Acknowledgements

This work was partially supported by the National Science Foundation (CHE1607554). Dr. Russell Hopson is thanked for assistance with NMR spectroscopy, and Adam Garlow is thanked for assistance with glycopolymer synthesis.

Notes and references

§ Baldisseri, D; Bruker Biospin. Practical Aspects of Fragment-Based Screening Experiments in TopSpin. Bruker BioSpin Technical Note

§§ The term epitope map, while derived from studies of antibody-antigen recognition, is used in STD-NMR experiments to refer to the relative STD effects of any small molecule ligand interacting with its receptor, proteinaceous or otherwise.

§§§ Control experiments confirmed that irradiation of 4-FPBA and 4-MPBA in the absence of a glycopolymer did not give rise to any STD effects (Figure S7).

§§§§ Similar to the observation with **3,5 DFPBA**, the ordering of the *ortho* and *meta* STD-AF_0 values is switched when the on-resonance saturation is carried out at 1.07 ppm (Figure S14)

1 R. Marchetti, S. Pérez, A. Ardá, A. Imberty, J. Jiménez-Barbero, A. Silipo and A. Molinaro, *ChemistryOpen*, 2016, **5**, 274–296.
2 L. Fielding, *Progress in Nuclear Magnetic Resonance Spectroscopy*, 2007, **51**, 219–242.
3 R. Ishima, *Appl NMR Spectrosc*, 2015, **1**, 143–181.
4 C. A. Lepre, J. M. Moore and J. W. Peng, *Chem Rev*, 2004, **104**, 3641–3676.
5 V. Friebolin, M. P. Bayer, M. T. Matyska, J. J. Pesek and K. Albert, *J. Sep. Sci.*, 2009, **32**, 1722–1728.
6 V. Friebolin, S. Marten and K. Albert, *Magn. Reson. Chem.*, 2010, **48**, 111–116.
7 Y. Suzuki, H. Shindo and T. Asakura, *J Phys Chem B*, 2016, **120**, 4600–4607.
8 H. Xu and L. B. Casabianca, *Sci. Rep.*, 2020, **10**, 1–8.
9 Y. Zhang, H. Xu, A. M. Parsons and L. B. Casabianca, *J. Phys. Chem. C*, 2017, **121**, 24678–24686.
10 F. De Biasi, D. Rosa-Gastaldo, X. Sun, F. Mancin and F. Rastrelli, *J Am Chem Soc*, 2019, **141**, 4870–4877.
11 J. Chen, J. Wang, Y. Bai, K. Li, E. S. Garcia, A. L. Ferguson and S. C. Zimmerman, *J Am Chem Soc*, 2018, **140**, 13695–13702.
12 J. C. Muñoz-García, R. Inacio Dos Reis, R. J. Taylor, A. J. Henry and A. Watts, *ChemBioChem*, 2018, **19**, 1022–1025.
13 M. Mayer and T. L. James, *J Am Chem Soc*, 2002, **124**, 13376–13377.
14 S. Di Micco, C. Bassarello, G. Bifulco, R. Riccio and L. Gomez-Paloma, *Angew. Chem. Int. Ed. Engl.*, 2006, **45**, 224–228.
15 F. A. Abulwerdi, W. Xu, A. A. Ageeli, M. J. Yonkunas, G. Arun, H. Nam, J. S. Schneekloth, T. K. Dayie, D. Spector, N. Baird and S. F. J. Le Grice, *ACS Chem Biol*, 2019, **14**, 223–235.
16 A. Szczygiel, L. Timmermans, B. Fritzinger and J. C. Martins, *J Am Chem Soc*, 2009, **131**, 17756–17758.
17 A. Fernandes, N. F. Brás, N. Mateus and V. De Freitas, *Langmuir*, 2014, **30**, 8516–8527.
18 S. Shahzad-ul-Hussan, R. Ghirlando, C. I. Dogo-Isonagie, Y. Igarashi, J. Balzarini and C. A. Bewley, *J Am Chem Soc*, 2012, **134**, 12346–12349.
19 A. N. Bristol, J. Saha, H. E. George, P. K. Das, L. K. Kemp, W. L. Jarrett, V. Rangachari and S. E. Morgan, *Biomacromolecules*, 2020, **21**, 4280–4293.
20 B. Meyer and T. Peters, *Angew. Chem. Int. Ed. Engl.*, 2003, **42**, 864–890.
21 G. Yilmaz and C. R. Becer, *Front Bioeng Biotechnol*, 2014, **2**, 39.
22 Y. Miura, Y. Hoshino and H. Seto, , 1673–1692.
23 L. L. Kiessling and J. C. Grim, *Chem Soc Rev*, 2013, **42**, 4476.
24 Chapter 1 in *Boronic Acids*, Ed. D. G. Hall, Wiley-VCH, 2005.
25 M. B. Espina-Benitez, J. Randon, C. Demesmay and V. Dugas, *Separation & Purification Reviews*, 2018, **47**, 214–228.
26 X.-T. Zhang, G. J. Liu, Z.-W. Ning and G.-W. Xing, *Carbohyd Res*, 2017, **452**, 129–148.
27 V. Spiwok, *Molecules*, 2017, **22**, 1038–11.
28 J. L. Asensio, A. Ardá, F. J. Cañada and J. Jiménez-Barbero, *Acc Chem Res*, 2013, **46**, 946–954.
29 R. Okoth and A. Basu, *Beilstein J. Org. Chem.*, 2013, **9**, 608–612.
30 M. Dowlut and D. G. Hall, *J Am Chem Soc*, 2006, **128**, 4226–4227.
31 N. DiCesare and J. Lakowicz, *Chem Commun*, 2001, 2022–2023.
32 F. Ferrage, K. Dutta and D. Cowburn, *Molecules*, 2015, **20**, 21992–21999.
33 W. Becker, K. C. Bhattiprolu, N. Gubensäk and K. Zangger, *ChemPhysChem*, 2018, **19**, 895–906.
34 M. Mayer and B. Meyer, *J Am Chem Soc*, 2001, **123**, 6108–6117.
35 N. B. Ley, M. L. Rowe, R. A. Williamson and M. J. Howard, *RSC Advances*, 2014, **4**, 7347–7351.
36 B. Claasen, M. Axmann, R. Meinecke and B. Meyer, *J Am Chem Soc*, 2005, **127**, 916–919.
37 J. Angulo and P. M. Nieto, *Eur Biophys J*, 2011, **40**, 1357–1369.
38 S. Monaco, L. E. Tailford, N. Juge and J. Angulo, *Angew. Chem. Int. Ed.*, 2017, **56**, 15289–15293.
39 V. Jayalakshmi and N. R. Krishna, *Journal of Magnetic Resonance*, 2002, **155**, 106–118.
40 G. Springsteen and B. Wang, *Tetrahedron*, 2002, **58**, 5291–5300.
41 J. Yan, G. Springsteen, S. Deeter and B. Wang, *Tetrahedron*, 2004, **60**, 11205–11209.
42 D. Zarzeczanska, A. Adamczyk-Woźniak, A. Kulpa, T. Ossowski and A. Sporzyński, *Eur. J. Inorg. Chem.*, 2017, **2017**, 4493–4498.
43 E. Bassil, *Plant Physiol*, 2004, **136**, 3383–3395.
44 R. Marchetti, M. J. Dillon, M. N. Burtnick, M. A. Hubbard, M. T. Kenfack, Y. Blériot, C. Gauthier, P. J. Brett, D. P. AuCoin, R. Lanzetta, A. Silipo and A. Molinaro, *ACS Chem Biol*, 2015, **10**, 2295–2302.
45 N. U. Tanoli, S. A. K. Tanoli, A. G. Ferreira, S. Gul and Z. Ul-Haq, *Med. Chem. Commun.*, 2015, **6**, 1882–1890.
46 K. L. Hudson, G. J. Bartlett, R. C. Diehl, J. Agirre, T. Gallagher,

L. L. Kiessling and D. N. Woolfson, *J Am Chem Soc*, 2015, **137**, 15152–15160.
47 S. Vandenbussche, D. Díaz, M. C. Fernández-Alonso, W. Pan, S. P. Vincent, G. Cuevas, F. J. Cañada, J. Jiménez-Barbero and K. Bartik, *Chemistry*, 2008, **14**, 7570–7578.
48 M. del Carmen Fernández-Alonso, F. J. Cañada, J. Jiménez-Barbero and G. Cuevas, *J Am Chem Soc*, 2005, **127**, 7379–7386.
49 J. M. Pollino and M. Weck, *Chem Soc Rev*, 2005, **34**, 193–15.
50 X. Zhang, T. Yuan, H. Dong, J. Xu, D. Wang, H. Tong, X. Ji, Bin Sun, M. Zhu and X. Jiang, *Colloid Polym Sci*, 2018, **296**, 1–13.
51 M. Gosecka and M. Gosecki, *Acta Biomater*, 2020, **116**, 32–66.